# Micro- and Nano-hierarchical Structures on Polymer Surfaces for Application to Super-hydrophobic Properties

**Hiroshi Ito#, Donghui Chu, Tetsuo Takayama, Kentaro Taki, Akihiko Nemoto**

Graduate School of Science and Engineering, Yamagata University, 4-3-16, Jonan, Yonezawa, Yamagata 992-8510, Japan
# Corresponding Author / E-mail: ihiroshi@yz.yamagata-u.ac.jp , TEL: +81-238-26-3081, FAX: +81-238-26-3081

KEYWORDS : hierarchical structure, anodized aluminum oxidation, mechanical tooling machine, nanoimprint, superhydrophobic

*This paper described the Superhydrophobicity of the transparent typical polymers, polycarbonate and polystyrene. These were patterned with nanorod and hierarchical structure which is combined nanorod with microconvex structures. Nanoporous structures were prepared by the anodized aluminum oxidation (AAO) which could precisely control the pore size and interpore size. The design parameters of nanoporous structures were controlled from 50nm to 250nm in pore diameter and 50nm to 100nm in interpore. Anodized aluminum oxide was done on the microstructures were fabricated with precise tooling machine. Micro-concave structures could be fabricated on the flat aluminum surfaces by using mechanical tooling process. The processing parameters were tuned to accurately achieve the desired geometries with various sizes. The fabricated polymer samples were prepared by thermal imprint process and then the effect of the different-sized structures on the water repellent properties was investigated in contact angle measurement with water.*

## 1. Introduction

Research conducted to elucidate superhydrophobic surfaces, which are defined as having a water contact angle greater than 150°, has revealed great interest in terms of fundamental study and fabrication methods because of the importance of these materials for application in practical fields such as water repellent windows, snow adhesion prevention, and anti-dust electronic devices[1-4]. The superhydrophobic property is governed mainly by chemical modification of the surface material and the surface roughness of hierarchical micro–nanostructures (cooperation of a nanostructure within the microstructure). A representative example in nature of a hierarchical surface with superhydrophobic properties is the lotus leaf[5-7]. The wetting property of hierarchical structures is explainable using well-known theories, such as Wenzel and Cassie–Baxter models for a liquid drop on rough solid surfaces. The contact angle of a water droplet is dependent on the ratio of trapped air-pocket in the solid–liquid interface. For hierarchical micro–nanostructures, the area fraction of solid surface contact with a liquid is much smaller than that of single-level structure; nanostructure or microstructure. It is explainable why hierarchical structures can generate a superhydrophobic state. Our research group has produced well-ordered hierarchical micro–nanostructures on polystyrene surfaces simply by the use of a thermal imprint machine. Microstructures on the mold inserts were prepared using a precision tooling machine[8]. These design parameters are controlled precisely during machining. Nanostructures were fabricated using anodized aluminum oxidation method.

This study examines systematic hierarchical micro–nanostructures which have highly ordered patterns and superhydrophobic properties using simple and large-scale fabrication methods.

## 2. Experiments

### *2.1 Fabrication of micro-, nano-, and hierarchical structure mold inserts*

Microstructures were fabricated on a flat aluminum sheet using a precision tooling machine (ROBONANO α-0iB ; Fanuc Ltd.). Concaved microball arrays were fabricated using a monocrystalline diamond needle having 35 μm tip diameter. The processing parameters were tuned to achieve the desired geometries accurately. Each concaved microstructure is inscribed with a groove motion of a tooling machine. The micropatterned surface area was 2 $cm^2$. Nano-structures were fabricated on aluminum surfaces with anodized aluminum oxide (AAO) processing. Preparation of anodic alumina on microstructured aluminum for a hierarchical micro–nano mold

insert is the same as the preparation of free-standing AAO processes. The high-purity aluminum sheet (99.99%) was degreased in acetone. Then it was electro-polished in a mixed solution of HClO4:H2O:EtOH=10:7:83. Electropolished aluminum sheets were anodized using two-step anodization. Anodization steps were performed individually at constant voltage of 40 V in 0.3 M oxalic acid, at 5°C for 24 hr. After finishing the first anodization, the porous alumina is dissolved selectively in a solution containing 0.6 M phosphoric acid and 0 M chromic acid, at 60°C. On the side on which the second anodization was done, the nanopores were opened by immersion in 5% H3PO4 solution at 30°C for 30 min. The backside of the anodized surface was removed in a saturated CuCl2 solution. Subsequently, the barrier layer was opened by chemical etching in 5 wt% phosphoric acid solution for 2 hr.

### *2.2 Fabrication of patterned polymer surfaces by nanoimprint*

Nano-, micro- and hierarchical structured polymer samples were prepared using a thermal nanoimprint machine (Izumi Tech., Japan). The commercial polymer, PS (polystyrene, MFR= at 200°C 5 kg, GPPS 679; PS Japan), was used as patterning. The polymer films were prepared using a commercial hot press machine. The prepared nano-, micro- and hierarchical masks were applied as mold inserts. The nanoimprint parameters are presented in Table 1. The anodic aluminum oxide was removed in a NaOH solution for 1 hr after nanoimprint molding.

### *2.3. Characterization of mold inserts and patterned polystyrene*

Images of mold inserts and patterned surfaces were observed using a scanning electron microscope (FE-SEM, SU-8000; Hitachi High-Technologies Corp.). The design parameters and replication ratios of microstructured parts in micro- and hierarchical micro–nano mold inserts were evaluated using laser spectroscopy (LEXT OLS 4000; Olympus Corp., Japan).

The sessile drop method was used for static and dynamic contact angle measurements of a commercial contact angle meter (DM 500; Kyowa Interface Science Co. Ltd., Japan). Deionized water (surface tension γlv = 72.1 mN/m), dispensed using a microsyringe, was used for liquid contact angle tests. The static contact angle was measured at four points for each sample. The average values were calculated. The experimental setup was in still air of 24±1°C with relative humidity of about 40±10%.

**Table 1. Thermal imprint parameters**

| | Mold Temperature (°C) | Melt time (min.) | Pressure (MPa) | Pressure time (min.) |
|---|---|---|---|---|
| **Micropatterned** | **120** | **5** | **0.2** | **5** |
| **Nanopatterned** | **120, 140** | **5** | **1** | **5** |
| **Micro-Nanopatterned** | **120, 140** | **5** | **1** | **5** |

## 3. Results and Discussion

### *3.1 Micro-, nano-, and hierarchical structures mold inserts*

The design parameters of the fabricated mold inserts are given as shown in Table 2. The notation of $M_x$, $N_y$, and $M_xN_y$ refers respectively to the number of mold inserts micro-, nano, and micro–nanostructures. Three micro-mold inserts were fabricated typically at different distances of microball structures 68.6 μm, 34.7 μm, and 10.8 μm. The other parameters, d and z, are set up with mutually similar values.

**Table 2. Dimensions of the mold inserts**

| | Mold insert | | |
|---|---|---|---|
| | **r [a]** | **d [b]** | **z [c]** |
| **$M_1$** | **36.3 μm** | **68.6 μm** | **26.6 μm** |
| **$M_2$** | **34.2 μm** | **34.7 μm** | **18.1 μm** |
| **$M_3$** | **30.6 μm** | **10.8 μm** | **18.5 μm** |
| **$N_1$** | **25 nm** | **50 nm** | **-** |
| **$M_1N_1$** | **36.2 μm, 25 nm** | **69.3 μm, 50 nm** | **25.7 μm** |
| **$M_2N_1$** | **34.2 μm, 25 nm** | **34.3 μm, 50 nm** | **17.6 μm** |
| **$M_3N_1$** | **30.8 μm, 25 nm** | **10.4 μm, 50 nm** | **18.3 μm** |

***r [a], diameter of microball or nanopore; d [b], inter microball or nano-pore distance; z [c], depth of microball***

The hierarchical micro-nano mold inserts show almost identical dimensions to those of the micro-mold and nano-mold inserts. Therefore, two-step anodizations on microstructured aluminum sheet rarely cause dimensional changes during self-ordered pore growth. Figure 1 presents a comparison of the microscale morphologies between the micro-mold inserts and hierarchical micro–nano mold inserts. Microstructured parts in hierarchical micro–nano mold inserts appear to be similar to the micro-mold inserts in all three mold inserts. However, unlike the hierarchical micro–nano mold inserts, some concaved microball structures showed flashes attributable to the aluminum ductility. These flashes could be dissolved along with the porous alumina layer, which is treated after the first anodization. Patterns that are replicas of the hexagonal pore array are preserved on the fresh aluminum surface, which allows the preparation of pores with high regularity by a subsequent second anodization under the same conditions as those of the first anodization. Comparison with the nano mold inserts reveals that the nanostructure part shows the same self-ordering pore arrays with a 25 nm diameter and 50 nm interpore distances. A profile of the microstructured AAO membrane slightly differs from that of the free-standing AAO membrane. Because nanopores grow perpendicular to the surface and because that direction is straight during anodization, the fan-shaped growth is attributed to the bent microstructure parts in hierarchical micro–nano mold insert.

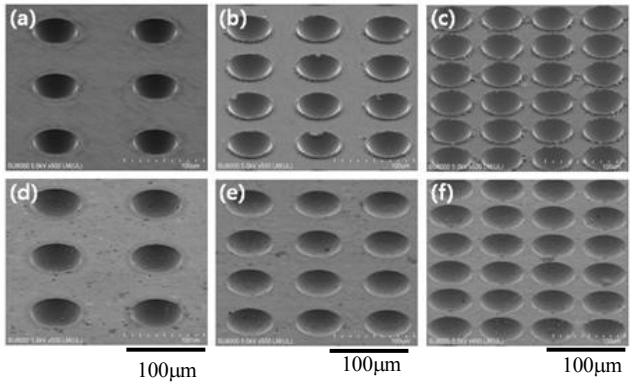


**Figure 1. SEM images of micro–nano and hierarchical micro–nano mold inserts: (a) mold insert $M_1$, (b) mold insert $M_2$, (c) mold insert $M_3$, (d) mold insert $M_1N_1$, (d) mold insert $M_2N_1$, (d) mold insert $M_3N_1$**

### *3.2 Dimensions of patterned polystyrene surfaces*

Polystyrene surfaces were patterned using micro-, nano-, and hierarchical micro–nano mold inserts in thermal imprint molding. The appropriate imprinting parameters were optimized for each structure. Typical images of hierarchical micro-nanostructures are depicted in Fig. 2. The SEM images of polystyrene surfaces show micrometer-sized convex structures that are exactly opposite from the image of the mold inserts presented in Fig. 1. At higher magnification, nanostructures on the micrometer-sized convex structure are visible short-nanorod (mold temperature 120°C) and long-nanorod (mold temperature 140°C) surfaces (Fig. 2). Increase of the nanorod length is shown with increasing imprint mold temperature. Furthermore, morphological disorder, arising from nanorod clustering, is shown at nanostructure parts it is increased at longer nanorod mold in 140°C (Figs. 2(g) and 2 (h)) because of the flexible characteristics of the polymer and the capillary forces created during evaporation of liquids[9], particularly in the case of long nanorods.

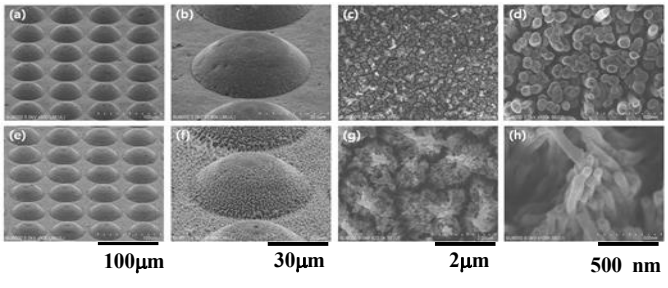


**Figure 2. SEM images of hierarchical micro-nanostructures on polystyrene surfaces replicated with mold inserts $M_3N_1$: (a) and (b) microstructure part molded at 120°C; (c) and (d) nanostructure part molded at 120°C; (e) and (f) microstructure part molded at 140°C; and (g) and (h) nanostructure part molded at 140°C**

From the SEM observation for all convex microstructures, M1, M2, and M3, show replication ratio higher than 95%, replicated at mold temperature 120°C in imprint process. We assumed that the mold temperature of 120°C sufficiently replicates the polymer surface and that it is sufficient to evaluate the apparent contact angle. All dimensions of the patterned polymer surfaces indicate almost identical values these of mold inserts. The length of nanorods shows higher values at higher temperatures because melted polymer flows readily into nanopore layers. Comparison of the two of mold temperature conditions, 120°C and 140°C, which are higher temperature conditions, indicates increased nanorod length: 490 nm to 1.1 μm in average values.

### *3.3 Hydrophobicity of patterned polystyrene surfaces*

Polystyrene surfaces were replicated using micro-, nano-, and hierarchical micro–nano mold inserts in a thermal imprint machine. Morphology and replication ratios of patterned polymer surfaces were evaluated using SEM, laser spectroscopy, and a contact angle meter; the results are shown in Fig. 3 and Table 3. Variation in the microstructures and nanostructures are shown respectively along the x- and y-axes in Fig. 3. Only microstructures are shown in the bottom-row series in the figure, which as developed with different area fraction. The apparent contact angle attained a maximum value of 129.8° at a highest area fraction of microstructure (replicated by M3 mold inserts), which is increased with 45% from the value of flat surface, 89.7° and decreased with lower area fraction. As described in our previous report[8], the contact angle on the patterned surface strongly depends on the area fraction ($\varphi_s$) of the solid surface as expressed using the Cassie – Baxter model[10]:

$$\cos\theta^* = -1 + \varphi_s(1 + \cos\theta) \qquad (1)$$

where $\theta$ and $\theta^*$ respectively represent the contact angles of a flat surface and rough surface, and $\varphi_s$ is the fraction of solid–liquid interface under the water droplet. Although a smaller $\varphi_s$ indicates a more hydrophobic property, our results revealed that the trapped air pockets were not sufficiently stable to support the water droplet increased with greater separation of microstructures. It is simultaneously affected by stability of trapped air pockets and surface energy property. However, as indicated on the left side of the column series in Fig. 3, where only nanostructures were developed on the flat polystyrene surface, the contact angle showed values of 126.5° and 134.5° (increased by 41% and 50% from flat surface values) molded at 120°C and 140°C, respectively. Although around 1 μm is an extremely short length of nanorod, it can display the high contact angle degree on the raw polymer surface because the nanorod structure has large free volume (surface area) between the nanorod and a very low contact area with water droplets. The effects of these nanostructures on the contact angle are maintained on the microstructures, hierarchical nano–micro structures as portrayed in Fig. 3. However, this effect is decreased slightly, probably because of the decrease of air pocket stability caused by the change of surface curvature. The highest contact angle on the hierarchical micro–nano

structured polystyrene surface was measured as superhydrophobic property, 150.6°, which shows a 68% increment from that of flat surface, where the contact angle values decrease with greater pitch size: 146.7° and 143.5° (i.e., 64% and 60%) at the mold temperature of 140°C.

**Table 3. Static contact angle of patterned polystyrene surfaces**

| | 120°C | 140°C |
|---|---|---|
| Flat [a] | 89.7° | |
| $M_1$ | 115.9° | - |
| $M_2$ | 123.8° | - |
| $M_3$ | 129.8° | - |
| $N_1$ | 126.5° | 134.5° |
| $M_1N_1$ | 133.0° | 143.5° |
| $M_2N_1$ | 136.6° | 146.7° |
| $M_3N_1$ | 140.9° | 150.6° |

**Flat [a]: prepared using commercial hot press machine at 180°C**

## 4. Conclusions

As described in this paper, we demonstrated a simple and effective method of producing polymer superhydrophobic surfaces replicated by hierarchical micro–nano mold inserts fabricated using a micro-manufacturing machine and anodized aluminum oxidation process. The water contact angle increased from 89.7° on the flat surface to greater than 150° on hierarchical polymer structures without additional coating.

## ACKNOWLEDGMENT

This research was financially supported by Cheil Industries Inc., Korea.

## REFERENCES

1. Bhushan B, Biomimetics: lessons from nature - an overview. Philos., Trans. R. Soc., A 367:1445−1486, 2009
2. Deng X, Mammen L, Butt HJ, Vollmer D, Candle Soot as a Template for a Transparent Robust Superamphiphobic Coating, Science 335(6064):67–70, 2012
3. Kako T, Nakajima A, Irie H, Kato Z, Uematsu K, Watanabe T, Hashimoto K, Adhesion and sliding of wet snow on a super-hydrophobic surface with hydrophilic channels, J. Mater. Sci. 39(2):547–555, 2004
4. Xue CH, Jia ST, Zhang J, Ma JZ, Large-area fabrication of superhydrophobic surfaces for practical applications: an overview. Sci. Technol., Adv. Mater. 11:1−15, 2010
5. Cortese B, D'Amone S, Manca M, Viola I, Cingolani R, Gigli G, Superhydrophobicity due to the hierarchical scale roughness of PDMS surfaces, Langmuir 24(6):2712−2718, 2008
6. Lee SM, Kwon TH, Effects of intrinsic hydrophobicity on wettability of polymer replicas of a superhydrophobic lotus leaf, J. Micromech. Microeng. 17:687−692, 2007
7. Sun M, Luo C, Xu L, Ji H, Ouyang Q, Yu D, Chen Y,Nonspherical colloidal crystals fabricated by the thermal pressing of colloidal crystal chips, Langmuir 21(19):8978–8991, 2005
8. Chu DH, Nemoto A, Ito H, Effects of geometric parameters for the superhydrophobicity with the polymer surfaces fabricated by precision tooling machine, Microsyst. Technol. 20, 193-200, 2014
9. Zhu K, Vinzant TB, Neale NR, Frank AJ, Removing structural disorder from oriented TiO2 nanotube arrays: reducing the dimensionality of transport and recombination in dye-sensitized solar cells, Nano Lett. 7(12):3739–3746, 2007
10. Cassie ABD, Baxter S, Wettability of porous surfaces, Trans. Faraday Soc. 40:546, 1944

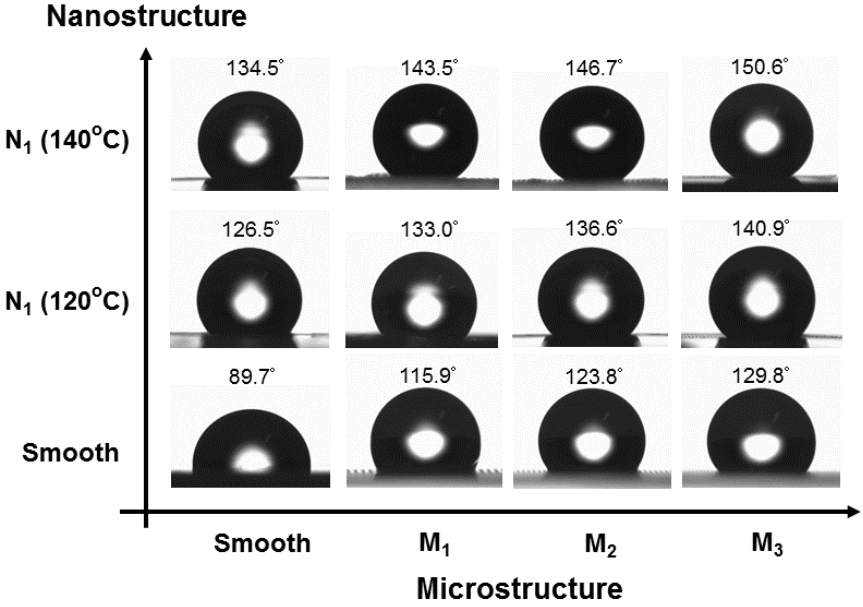


**Figure 3. Water contact angles of patterned polystyrene surfaces (x-axis shows the mold inserts of microstructures and y-axis shows the mold temperature of nanostructures)**